Structure and function of type I copper in multicopper oxidases

Review

Structure and function of type I copper in multicopper oxidases

T. Sakurai* and K. Kataoka

Graduate School of Natural Science and Technology, Kanazawa University, Kakuma, Kanazawa 920-1192 (Japan),

Fax: +81-76-264-5742, e-mail: ts0513@kenroku.kanazawa-u.ac.jp

Address correspondence to

Takeshi Sakurai

Graduate School of Natural Science and Technology, Kanazawa University, Kakuma, Kanazawa 920-1192, Japan

Tel: +81-76-264-5685

Fax: +81-76-264-5742

e-mail: ts0513@kenroku.kanazawa-u.ac.jp

Running title: Type I copper of multicopper oxidase

Abstract. The type I copper center in multicopper oxidases is constructed from 1Cys2His and weakly coordinating 1Met or the non-coordinating 1Phe/1Leu, and it exhibits spectral properties and an alkaline transition similar to those of the blue copper center in blue copper proteins. Since the type I copper center in multicopper oxidases is deeply buried inside the protein molecule, electron transfers to and from type I copper are performed through specific pathways: the hydrogen bond between an amino acid located at the substrate binding site and a His residue coordinating type I copper, and the His-Cys-His sequence connecting the type I copper center and the trinuclear copper center comprised of a type II copper and a pair of type III coppers. The intramolecular electron transfer rates can be tuned by mutating the fourth ligand of type I copper. Further, mutation at the Cys ligand gives a vacant type I copper center and traps the reaction intermediate during the four-electron reduction of dioxygen.

Keywords. Type I copper, trinuclear copper center, multicopper oxidase, blue copper protein, CueO, laccase, bilirubin oxidase.

*Corresponding author

Introduction

Nearly all organisms utilize copper as an essential trace element. Biological roles of copper include electron transfer, oxidation of organic substrates and metal ions, dismutation of superoxide, monooxygenation, transport of dioxygen and iron, and reduction of dioxygen, nitrite and nitrous oxide etc [1]. These functions of copper parallel those of iron due to their shared redox active properties. Regarding oxidation state, copper(I) and copper(II) states are utilized in biological systems, while the involvement of the copper(III) state has been erroneously suggested for galactose oxidase.

Copper in proteins has been classified into three groups based on their spectroscopic and magnetic properties: type I copper, type II copper, and type III copper. Type I copper shows intense absorption at around 600 nm and narrow hyperfine splittings in the electron paramagnetic resonance (EPR) spectroscopy. Type II copper does not give strong absorption at 600-700 nm and shows hyperfine splittings of the normal magnitude in the EPR spectrum. Unlike type I copper and type II copper, type III copper is not detected in the EPR spectrum because of strong antiferromagnetic interaction. This classification of copper has been based on coppers contained in lacquer laccase, the prototype multicopper oxidase (MCO). On the other hand, copper in proteins containing only one type of copper has been classified into blue copper, non-blue copper or EPR non-detectable copper. These coppers have also been extensively called type I copper, type II copper, and type III copper, respectively.

Blue copper protein is a class of copper proteins containing only a blue copper center in a relatively small-sized protein molecule of 9 to 23 kDa that functions in electron transfer [2-4], although the subgroup called phytocyanin in higher plants is considered to function as a radical scavenger. Red copper protein (nitrosocyanin) is a variant of blue copper protein with a modified ligand set (*vide infra*) [5]. (Table 1 lists the copper proteins containing the blue copper center and the type I copper center and their variants). Basically the same copper center, type I copper, is also present in MCOs containing four copper centers: a type I copper and a trinuclear copper center comprised of a type II copper and a pair of type III copper's [6-8].

The function of both the blue copper center and the type I copper center is electron transfer.

Since MCO is an oxidase, the electron transfer pathways to and from type I copper are different: electrons withdrawn from the substrate are transferred to the trinuclear copper center via type I copper and are used to convert dioxygen to water. On the other hand, blue copper proteins shuttle an electron between exogenous redox partners through the coordinating His imidazole group, although the directional electron transfer occurs in plant plastocyanin located on the thylakoid membrane surface [9,10] and only putatively occur in amicyanin.

Copper-containing nitrite reductase (NIR) involved in the anaerobic respiration system is a subgroup of MCOs, which contains a type I copper and a type II copper [11]. The type I copper in NIR is used for entry of electrons from a blue copper protein or cytochrome *c*. The type II copper in NIR is used as a binding and reducing site for substrates. Nitrous oxide reductase (N_2OR) and cytochrome *c* oxidase (COX) have a binuclear copper center, Cu_A, which is a variant of type I copper and iron-sulfur center and functions to facilitate entry of electrons towards the reduction centers of nitrous oxide (Cu_Z) and dioxygen (heme a_3-Cu_B), respectively [12].

In the present article, we review the structure and function of type I copper in MCOs and their variants in comparison with those of blue copper proteins and their variants. While a number of excellent reviews on blue copper proteins are available [2-4,13-16], type I copper with extensive biological features has not been reviewed yet.

Structure of the type I copper center in multicopper oxidases

The ligand groups commonly coordinating the blue copper center and the type I copper center in MCO are 1Cys and 2His residues (Figure 1, Table 1). Met is widely utilized as the fourth ligand, although the electron-donating ability of the thioether group is considerably low compared to the cysteinate sulfur and the imidazole nitrogen [2,16]. In phytocyanins from higher plants, however, Met is replaced by Gln containing an amide group in the side chain with a stronger electron-donating ability compared to the thioether group in the side chain of Met. The fourth ligand for the type I copper center is not present in fungal laccases, in which the uncoordinating Phe or Leu occupies the position [5-7]. An amide carbonyl group in the main chain approaches the blue copper center in azurin

with a distance of ca. 3 Å [17-22]. Figure 2 compares the structure and properties of the type I copper center and the blue copper center together with their variants, the red copper center with the coordination of 1Cys2His1Glu and a water molecule [5], and the coupled Cu_A center in N_2OR and COX [23-25].

Most of the blue copper proteins plastocyanin, azurin, pseudoazurin, amicyanin, rusticyanin, auracyanin, umecyanin, mavicyanin, plantacyanin (cucumber basic protein (CBP)), and stellacyanin have been crystallized and their structural data are available [4,16]. On the other hand, crystal structure analyses of MCOs comprised of more than 500 amino acids have been limited until recently. However, crystal data are now available for fungal laccases from *Coprinus cinereus* [26,27], *Trametes versicolor* [28, 29], *Melanocarpus albomyces* [30, 31], *Rigidoporus lignosus* [32], and *Cerrena maxima* [33], CotA [34-36], CueO [37-39], Fet3p [40], phenoxazinone synthese [41], ascorbate oxidase [42,43], and ceruloplasmin [44,45] (Table 2), although plant laccase, bilirubin oxidase, PcoA, manganese oxidases such as CumA and MnxG, dihydrogeodin oxidase, and hephaestin have not been crystallized yet. The difficulty in crystallizing lacquer laccase, the prototype MCO, comes from its high sugar content of ca. 50%. An expression system to obtain sugar free lacquer laccase has not been constructed yet. The type I copper in MCO is coordinated by 1Cys2His1Met except for the fungal laccases and Fet3p, in which Phe or Leu occupies the position of Met. Crystal structure analysis of reduced MCO has been performed for only ascorbate oxidase, indicating that the space formed by the trinuclear copper center becomes wide to accommodate dioxygen [42]. Crystal structure analyses of ascorbate oxidase [42], CotA [35] and *T. versicolor* laccase [29], to which substrates or inducers were bound (*vide infra*), demonstrated that the structure around the type I copper center was not noticeably perturbed upon binding of the substrate or inducer.

The MCO molecule consists of three domains, each of which has a folding analogous to that of cupredoxin (blue copper protein) [28,29] (Figure 3). The trinuclear copper center is located at the interface of domain 1 and domain 3, and the type I copper center at domain 3, being further from the protein surface when compared to the blue copper center in blue copper proteins. An exception to the general molecular structure of MCOs is ceruloplasmin. Ceruloplasmin consists of six domains: three repetitions of the two-domain unit [44-46]. This two-domain structure [47] is considered to be an

ancient form of MCO from which the three-domain MCO evolved [11]. Two type I copper centers constructed from 1Cys2His1Met (domains 4 and 6) and one type I copper center constructed from 1Cys2His1Leu (domain 2) are present in ceruloplasmin, although only one trinuclear copper center is present at the interface between domains 1 and 6 [44,45]. NIR, whose structure is a homo-trimer of two-domain monomers [48,49], evolved from the common ancestor with ceruloplasmin.

Figure 4 shows the structure of the copper site in a MCO, CueO (A) [37], together with those of NIR (C) [49] and mavicyanin (B) [50]. The backbone peptides show how the ligand amino acids are connected to each other. The architecture of the type I copper center and the blue copper center are analogous in that Cys, His and Met/Gln are located in a loop and only another His is in the other loop. Type I copper is connected to type III coppers through the His-Cys-His sequence in MCO and with type II copper though the His-Cys sequence in NIR. Further, a peptide chain harboring the His ligands for type I copper and type II and III coppers (MCO) or type II copper (NIR) (magenta in Figures 4A and 4C) indirectly connects the Cu sites separated by ca. 13 Å. The copper-ligand bond distances have been tabulated in the literature [16]. The structure of type I copper in most MCOs is trigonal pyramidal or distorted tetrahedral as in many blue copper proteins, but trigonal planar in fungal laccases and Fet3p (Figure 2).

Spectroscopic properties of the type I copper center in multicopper oxidases

Absorption and circular dichroism (CD) spectra

The absorption spectral features of MCO are similar to those of blue copper proteins except for the presence of a band at ca. 330 nm derived from the trinuclear copper center, since the contribution from type I copper is significant over a wide range of wavelengths (Figure 5A, absorption spectra of CueO and azurin). The band at around 600 nm originating from the charge transfer Cys(S_π^-) $\rightarrow$ Cu^{2+} is most peculiar (ε = 4500 ~ 6000) [2-4,6-8] and accordingly, MCO is also called blue oxidase. The band at around 700-850 nm is now assigned to the d-d transitions as in the case of blue copper proteins. The band at ca. 450 nm assigned to the His(N) $\rightarrow$ Cu^{2+} charge transfer is considerably weak for every MCO, although its intensity is considerably strong for blue copper proteins showing the

rhombic EPR signal. Copper-containing NIR molecules are classified into blue and green groups due to their relative absorption intensities at 450 and 600 nm [51,52]. The Leu→His variant of a fungal laccase showed changes in type I copper from the blue site to the green site [53], while the Leu→Phe mutant did not show any notable change [54]. MCO mutants prepared hitherto are listed in Table 3.

In contrast to the absorption spectrum, the CD spectrum of MCO (Figure 5B) is considerably complex. The sign of the charge transfer band at around 600 nm, $Cys(S_{\pi}^{-}) \rightarrow Cu^{2+}$, is positive in MCOs containing type I Cu with Met as the fourth ligand, but is negative in fungal laccases containing the three-coordinated type I Cu [55]. The charge transfer band, $Cys(S_{\sigma}^{-}) \rightarrow Cu^{2+}$ affords a shoulder at ca. 530 nm, although its presence is not recognized from the absorption spectrum. Oppositely signed bands coming from $His(N) \rightarrow Cu^{2+}$ and $Met(S) \rightarrow Cu^{2+}$ are observed at 400-500 nm, while the latter band sometimes becomes noticeable when performing curve analysis. In contrast to the blue copper center and type I copper center with distorted tetrahedral or trigonal pyramidal structures and short Cu-S^{-}(Cys) bonds (1.95-2.16 Å), the red copper center in nitrosocyanin from *Nitrosomonas europaea* with a square pyramidal structure and a longer Cu-S^{-}(Cys) bond (2.26 Å) shows an intense absorption band at 390 nm (ε = 4400) [5].

The d-d bands of type I copper give a considerably strong negatively-signed CD band at around 800 nm, masking the contributions from d-d bands of type II and III coppers. These bands are observable in only the Cys to Ser mutant of the type I copper center in bilirubin oxidase [56], Fet3p [57] and CueO (unpublished) (*vide infra*). By mutating an Asp residue as a potential proton donor for dioxygen, which is positioned behind the trinuclear copper center, absorption at 330 nm was affected, although the band at 600 nm did not change [58]. Contributions from the trinuclear copper center to the CD spectrum at around 330 nm are not usually significant except for in CueO, since the OH^{-} group bridged between the type III coppers does not intrinsically have an asymmetric character.

Cu_A in N_2OR is in the mixed-valence state, S = 1/2 [Cu(1.5)•••Cu(1.5)], and shows predominant S^{-}(Cys) → Cu^{2+} charge transfer bands at ~480 nm and 530 nm, as well as a class III mixed valence charge transfer band around 800 nm [59]. The magnetic circular dichroism (MCD) spectrum is similar to that of bovine heart COX [60], in which the contributions from the Cu_A center to the absorption spectrum are masked by the contributions from three heme centers.

EPR spectra

In the EPR spectra of MCOs both signals derived from type I copper and type II copper have been detected [6,7] (Figure 5C). Type I copper gives a signal with axial symmetry and the hyperfine splitting of A_{II} ~ 10 x10^{-3} cm^{-1}. The rhombic type I copper signal as observed in blue copper proteins with the coordination of Gln, has not been reported in authentic or recombinant MCOs, although it has been artificially obtained in the Met → Gln mutants of bilirubin oxidase [56,61], CueO (unpublished) and NIR [62]. Mutations of Met → Phe/Leu for bilirubin oxidase (unpublished), CueO (unpublished) and CotA [63] resulted in the type I copper with the coordination found in fungal laccases, but the artificially prepared type I copper site became unstable due to the loss of a coordinating group. The modified type I copper site was not fully occupied with copper atoms, giving weakened EPR signal intensities. The mutation of Met → Gly for bilirubin oxidase [64] led to a decrease in the A_{II} value and increase in the g_{II} value, which is comparable to the change reported for mutations of the blue copper protein. The mutations of Phe/Leu → Met in fungal laccases also led to slight modifications in the EPR signal [65]. Since the type I copper and type II copper signals overlap in the EPR spectra of MCOs, simulations have been performed to determinate the spin Hamiltonian parameters of type II copper. Another striking feature of the EPR spectra of MCO is that an uncoupled type III copper signal is occasionally observed for isolated recombinant MCOs [56,61]. This takes place because the recombinant MCOs have not experienced a turnover and are in a state differing from that of the resting authentic MCO [66].

The red copper center gives an EPR signal more similar to normal copper (A_{II} = 13.8 mT) due to the coordination of Glu [67]. The Cu_A center of N_2OR and COX shows seven-line hyperfine splitting in the g_{II} regions of the EPR signal, indicating that two copper centers interact magnetically [68].

Resonance Raman Spectra

The resonance Raman spectrum of MCO has not been studied in detail. Only the data for the resting MCOs and some mutants with excitations at their 600 nm band are available [69-71]. Their spectral

features are very similar to those of blue copper proteins in that they have the clustered bands due to the mixing of the metal–ligand stretching. The Raman shifts of the clustered bands decrease on the order Phe/Leu/Gly (vacant), Met, and Gln for the fourth ligand. Fluorescence does not allow excitation at the 330 nm band. The UV resonance Raman spectrum has also not been reported yet. The resonance Raman spectrum of N_2OR in three oxidation states (oxidized, semi-reduced, and reduced) discriminated the contribution from Cu_Z and Cu_A sites, showing vibrational modes between 220 and 440 cm^{-1} [72].

X-ray absorption spectra

K-edge and extended X-ray absorption fine structure (EXAFS) spectra of MCOs have also not been widely measured. Since contributions from each copper site overlap, the average copper-copper distance in the trinuclear copper center can be obtained. The EXAFS spectra of the type II copper-depleted laccase [73] and ascorbate oxidase [74] show that their type III coppers are in the cuprous state even under air and are therefore different from the coupled copper centers in hemocyanin and tyrosinase. The EXAFS spectrum of Cu_A in N_2OR was very similar to that of COX and a copper-copper distance of ca. 2.4 Å was determined [75].

Properties of type I copper in multicopper oxidases

Redox potentials of the copper centers in MCOs have been determined by measuring the absorption spectrum and potential of the partly reduced states of MCO *in situ* [6,16,76-78]. The redox potential of type I copper ranges over ca. 360 – 780 (>1000) mV, which are higher redox potentials compared to those of blue copper proteins (184 – 680 mV) and red copper protein (+85 mV) (Table 1). The redox potentials of type II copper and type III copper have been measured by changes in the EPR signal intensity of type II copper and the absorption at 330 nm, respectively.

The redox potential of type I copper in some MCOs has also been measured electrochemically [79-84], although a molecular mass higher than 50 kDa is exceptionally unfavorable for obtaining clear electrochemical responses. Direct electrochemistry using pyrolytic graphite as a working

electrode or mediated electrochemistry using Au electrodes modified with an appropriate promoter by self assembly permit the measurement of the redox potential of type I copper, when the MCO molecules take the appropriate orientation on the electrode surface and electric communication between the electrode and type I copper becomes possible. Thus, the redox potential of the type I coppers of plant and fungal laccases [80], ascorbate oxidase [79], bilirubin oxidase [81,84], CeuO [83] have been electrochemically determined, although the association of these proteins and the electrode sometimes gave slightly different values from those determined by the titration method. The shorter the distance of type I copper from the protein surface, the better the electrochemical response. However, since the type I copper site in MCO is located under the substrate-binding cleft, the electrochemistry of MCO is unfavorable compared to blue copper protein, in which the imidazole edge of the His ligand is exposed on the flat protein surface [85-88]. In the case of NIR, the electrochemical communication of type I copper with the electrode was effectively performed by using an Au electrode modified with a promoter [89] and still more effectively by using mediator proteins such as azurin and pseudoazurin, thus affording an analytical method to measure enzyme activity [90]. Figure 6 schematically illustrates these electrochemical processes of MCOs.

Blue copper proteins show a so-called “alkaline transition” of their absorption wavelength, absorption intensity, and redox potential [91-94]. With increasing pH, especially at pH 8-11, the absorption maximum at ca. 600 nm shifts to shorter wavelengths and its absorption intensity decreases with the concomitant redox potential shifts to negative values. In some cases, the changes give sigmoidal curves, suggesting the involvement of deprotonation of amino acids [95]. Therefore, it has been suggested that deprotonation of a coordinated imidazole group or an amino acid hydrogen-bonded with a coordinated group [50] is the cause the alkaline transition, although it has not been evidenced yet. Rather, negative data has been obtained from mutation studies (unpublished).

The alkaline transition of MCO has not been studied in detail but we have recently reported that bilirubin oxidase shows a dramatic alkaline transition [96]. With increasing pH values higher than 7, the characteristic blue color faded reversibly and the intensity of the type I copper EPR signal also changed concomitantly with the absorption change. “Autoreduction” is supposed to be derived from a shift in the equilibrium between Cu^{2+}-S^{-} and Cu^{+}-$S^{\bullet}$ depending on the pH [94]. When the radical

center is delocalized on the sulfur atom, copper is formally in the cuprous state and $S^{\bullet}$ may not give an EPR signal because of broadening. If protein deformation is the cause of the alkaline transition of blue copper protein and MCO, it would be difficult to explain why common changes take place. More information about the reduced state of MCO is required to understand the alkaline transition intrinsic to the blue copper center and the type I copper center.

Function of type I copper in multicopper oxidases

The function of type I copper in MCO is to withdraw an electron from the substrate and transfer it to the trinuclear copper center. This becomes possible because the redox potential of the substrate is more negative than that of type I copper (Figure 7). When the Met ligand of the type I copper in bilirubin oxidase was replaced with Gln, the redox potential of type I copper shifted negatively by ca. 200 mV, giving rhombic type I copper EPR signal [56,61,70,81,84]. Enzyme activity for organic substrates dramatically decreased since the electron transfer from the substrate to type I copper became thermodynamically uphill, although the driving force for the succeeding electron transfer process from type I copper to the trinuclear copper center became steeply downhill. In connection with this, the ferroxidase activity of the Gln mutant increased more than 150% compared to the wild-type enzyme. An analogous negative shift in the redox potential, a spectral change related to type I copper, and a decrease in activity have all been observed in the Met150Gln mutant of NIR (62). On the other hand, when Met was substituted with Phe and Leu, the redox potential of type I copper in CotA [63], bilirubin oxidase (unpublished), and CueO (unpublished) increased as in the case of fungal laccases with a concomitant decrease in the enzyme activities. Met $\rightarrow$ Phe and Leu mutations of the type I copper ligand in bilirubin oxidase led to the possible coordination of an Asn residue located adjacently to the type I copper site. This occurred in order to prevent the unstable three-coordinate state of copper. The crystal structure analysis of Met $\rightarrow$ Phe/Leu mutants of CotA [63] demonstrated that the protein structure became considerably unstable and the type I copper center was not fully occupied as in the cases of bilirubin oxidase and CueO. Therefore, the type I copper center in MCO might also contribute to increase stability of the protein structure. The Phe and Leu mutants showed

prominent reductions in enzyme activities because the electron transfer between type I copper and the trinuclear copper center became unfavorable as illustrated in Figure 7. Effects of mutations at the trinuclear copper center and the putative proton donor concerned in the four-electron reduction of dioxygen have been reviewed elsewhere [8].

The electron transfer processes of MCOs and NIR from the substrate to type I copper and from type I copper to the catalytic center have been studied with the stopped-flow technique, flash-photolysis, and pulse-radiolysis [37,51,52,97-106]. The initial electron transfer process from the substrate to type I copper involves the association of substrate with the protein molecule, and accordingly, the proper selection of the substrate is extremely important to study the initial electron transfer process. Unlike the initial stage of the MCO reaction, the succeeding intramolecular electron transfer pathway from type I copper to the trinuclear copper center and the four-electron reduction of dioxygen [56,102,103] are not affected by how the reaction is started, although these processes will be accelerated under steady state conditions in the presence of excess substrate [101].

The electrochemistry of MCO also involves the preceding association of the protein molecule with the electrode surface and electron transfer from the electrode to type I copper. The electrochemistry of the Met $\rightarrow$ Gln mutant of bilirubin oxidase indicated that the intramolecular electron transfer between the type I copper center and the trinuclear copper center were accelerated as expected from the change in redox potential [84]. The electric current density due to the electron transfer between the electrode surface and type I copper of fungal laccases [80,82], bilirubin oxidase [81,84] and CueO [83] dramatically increased in the presence of dioxygen, since dioxygen was effectively converted to water without forming activated oxygen species. CueO was found to be the most promising cathodic catalyst to construct a biofuel cell because of high stability and high electric current density. If the biofuel cell is used at pH 7, it is ideal that type I copper of MCO has a redox potential slightly lower than 0.815 mV, the potential at which dioxygen is converted to water. If MCO effectively functions at a more acidic pH, a higher voltage would be expected. MCOs that show more positive potentials have been explored in order to obtain larger voltage differences between the anodic catalyst and the cathodic catalyst.

The electron transfer from the type I copper center to the trinuclear copper center passes

through the His-Cys-His triad. The electron transfer is performed using the through-bond mechanism, although a hydrogen bond between the O of Cys507 and the N^{δ} of His506 has been considered to be a short path in the case of ascorbate oxidase [100]. Therefore, the possible two electron transfer pathways leading to type III coppers might not be equivalent. In addition, it has been considered that the presence of the oxygen complexes significantly favors intramolecular electron transfer by affecting the driving force (i. e. redox potential) [101].

Substrate specificity of multicopper oxidases

The specific binding of substrate and the electron transfer to the type I copper center is a process in which MCO functions as an oxidase. Unlike this process, which is specific to each MCO, the subsequent processes that transfer electrons from type I copper to the trinuclear copper center and convert dioxygen to water commonly take place in every MCO.

The substrate specificity of MCOs is considerably broad except for the metallo-oxidases such as CueO, Fet3p, ceruloplasmin and manganese oxidases. Organic substrates are bound to the cleft at the "north" side of the protein molecules constructed by loops attached to the β-barrel scaffolds of the MCO domains (Figure 3). The shape of the cleft is one of the critical factors that produce substrate specificity in MCOs. Bulky laccase substrates such as 2,2'-azinobis(3-ethylbenzothiazoline-6-sulfonic acid) (ABTS) and syringaldazine were found to bind to the cleft of the substrate binding site in its folded form as indicated by X-ray crystallography of CotA [35] and the substrate-docked model of bilirubin oxidase [7]. An acidic amino acid is hydrogen-bonded with an imidazole group coordinating to type I copper, forming the electron transfer pathway. The side chain of Asp206 directly interacted with the 2,5-xylidine used as an inducer in the crystal structure of *T. versicolor* laccase [29]. Accordingly, the Asp residue must be one of the key amino acids to produce laccase activity, giving a bell-shaped activity profile depending on pH. In the case of ascorbate oxidase, the two OH groups of L-ascorbate were within hydrogen-bonding distance of the imidazole nitrogen (NE2) of His512 coordinated to type I copper and the indole nitrogen (NE1) of Trp362 [42]. A stacking interaction of the L-ascorbate ring with the aromatic ring of another Trp also facilitated the

binding of the substrate. Thus, the substrate specificity of MCO for organic substrates is produced by the integrated effect of the shape of the substrate-binding site and non-covalent interactions of the substrate with the amino acid(s) adjacent to the His residue coordinating to type I copper.

In contrast, cuprous oxidase, CueO, and ferroxidases, Fet3p and ceruloplasmin constitute their specific copper- or iron-binding site by assembling the ligand amino acids 2Asp2Met [37,38] (Figure 4), 1Glu2Asp1Gln [40], and 2Glu1Asp1His [44,45], respectively and affording a proper lability to the substrate metal ions. The substrate-binding site of CueO is insulated from bulk water by 50 amino acids including helices 5-7 [107]. Full and partial deletions of this segment produced oxidizing activities for a variety of laccase substrates depending on the extent of the deletion, affording evidence that helices 5-7 are essential for CueO to function as a cuprous oxidase. One of the Asp residues used as a ligand for the substrate is hydrogen-bonded with a His ligand coordinating type I copper, and thereby constructs the electron transfer pathway (Figure 4) [37,38]. An analogous hydrogen bond also has been found in Fet3p [40] and ceruloplasmin [44,45]. This hydrogen bond is a universal contrivance to realize prompt electron transfer from the substrate to type I copper, which is buried inside the protein molecule.

In the case of NIR, the association with the redox partner is extremely important. The north side of NIR that accepts electrons from the cognate partner, blue copper protein (pseudoazurin, azurin) or cytochrome *c*, has a hydrophobic flat docking surface [48, 49]. In addition to the hydrophobic interactions, the fact that electrostatic interactions are also important for formation of a productive electron transfer complex between NIR and pseudoazurin, has been demonstrated by performing mutant preparations [125, 133], crystal structure analysis [134], and computational simulation [135].

Concluding remarks

The structure and properties of the type I copper center in MCO and NIR show a marked resemblance to the blue copper center in blue copper protein, while the type I copper center is closely connected with other copper site(s) through the amino acids intervening between them. The electron donor for type I copper is an organic substance or metal ion in the case of MCO and a protein molecule such as

blue copper protein or cytochrome *c* in the case of NIR. Therefore, the specific binding site of the substrate is adjacent to the type I copper center, and the electron transfer pathway is formed between the substrate binding site and the type I copper center by the hydrogen bond between an acidic amino acid and one of the His residues coordinating type I copper. The subsequent long–range electron transfer to the catalytic center is performed through the amino acids separating the type I copper center and the catalytic center. Mutations at or around the type I copper center change its redox potential and substrate specificity, leading to modifications of the oxidase function of MCO and to the development of MCO as an electro-catalyst for biofuel cells and a catalyst for dye formation and bleaching.

Acknowledgement. This work was supported by a Grant-in-Aid for Scientific Research from the Ministry of Education, Science, Culture and Sports, Japan (19350081 to ts), NEDO, Toyota Motor Corporation, and Mandom Corporation.

1. Frausto da Silva J. J. R. and Williams R. J. P. (2001) The biological chemistry of the elements. The inorganic chemistry of life. 2nd ed. Oxford University Press, Oxford
2. Solomon E. I., Szilagyi R. K., George S. D. and Basumallick L. (2004) Electronic structures of metal sites in proteins and models: contributions to function in blue copper proteins. Chem. Rev. **104:** 419-458
3. Vila A. J. and Fernandez C. O. (2001) Copper in electron-transfer proteins. In: Handbook on metalloproteins. pp. 813-856, Bertini I., Sigel A. and Sigel H. (eds.), Marcel Dekker, New York
4. Messerschmidt A., Huber R., Poulos T. and Wieghardt K. (eds.) (2001) Cupredoxins (type-1 copper proteins). In: Handbook of metalloproteins, vol. 2. pp. 1151-1241, John Wiley & Sons, Chichester
5. Lieberman R. L., Arciero D. M., Hooper A. B. and Rosenzweig A. C. (2001) Crystal structure of a novel red copper protein from *Nitrosomona europaea*. Biochemistry **40:** 5674-5681
6. Messerschmidt A. (ed.) (1997) Multi-copper oxidases, World Scientific, Singapore
7. Solomon E. I., Sundaram U. M. and Machonkin T. E. (1996) Multicopper oxidases and oxygenases. Chem. Rev. **96:** 2563-2605
8. Sakurai T. and Kataoka K. (2007) Basic and applied features of multicopper oxidases, CueO, bilirubin oxidase and laccase. Chem. Rec. in press
9. Guss J. M. and Freeman H. C. (1983) Structure of oxidized popular plastocyanin at 1.6 Å resolution. J. Mol. Biol. **169:** 521-563
10. Mussiani F., Dikiy A., Semenov A. Y. and Ciurli S. (2005) Structure of the intermolecular complex between plastocyanin and cytochrome *f* from spinach. J. Biol. Chem. **280:** 18833-18841
11. Nakamura K. and Go N. (2005) Function and molecular evolution of multicopper blue proteins. Cell. Mol. Life. Sci. **62:** 2050-2066
12. Kroneck P. M. H. (2001) Binuclear copper A. In: Handbook of metalloproteins. vol. 2. pp. 1331-1341, Messerschmidt A., Huber R., Poulos T. and Wieghardt K. (eds.), John Wiley & Sons, Chichester

13. De Rienzo F., Gabdoulline R. R., Wade R. C., Sola M. and Menziani M. C. (2004) Computational approaches to structural and functional analysis of plastocyanin and other blue copper proteins. Cell. Mol. Life. Sci. **61:** 1123-1142

14. Nerssisian A. M. and Shipp E. L. (2002) Blue copper-binding domains. Adv. Protein Chem. **60:** 271-340

15. Machczynski M. C., Gray H. B. and Richards J. H. (2002) An outer-sphere hydrogen-bond network constrains copper coordination in blue proteins. J. Inorg. Biochem. **88:** 348-380

16. Gray H. B., Malmstrom B. G. and Williams, R. L. (2000) Copper coordination in blue proteins. J. Biol. Inorg. Chem. **5:** 551-559

17. Li C., Inoue T., Gotowda M., Suzuki S., Yamaguchi K., Kataoka K. and Kai Y. (1998) Structure of azurin-I from the denitrifying bacterium *Alcaligenes xylosoxidans* NCIMB 11015 at 2.45 Å resolution. Acta Crystollogr. Sect. D **54:** 347-354

18. Dodd F. E., Hasnain S. S., Abraham Z. H. L., Eady R. R. and Smith B. E. (1995) Structure of a new azurin from the denitrifying bacterium *Alcaligenes xylosoxidans* at high resolution. Acta Crystollogr. Sect. D **51:** 1052-1064

19. Nar H., Messerschmidt A., Huber R., van de Kamp M. and Canters, G. W. (1991) Crystal structure analysis of oxidized *Pseudomonas aeruginosa* azurin at pH 5.5 and pH 9.0. J. Mol. Biol. **221:** 765-772

20. Lee H., Dahms T., Ton-That H., Zhu D.-W., Biesterfeldt J., Lanthier P. H., Yaguchi M. and Szabo A. G. (1997) Primary sequence and refined tertiary structure of *Pseudomonas fluorescens* holo azurin at 2.05 Å. Acta Crystollogr. Sect. D **53:** 493-506

21. Baker E. N. (1988) Structure of azurin from *Alcaligenes denitrificans*. J. Mol. Biol. **203:** 1071-1095

22. Chen Z.-W., Barber M. J., McIntire W. S. and Mathews F. S. (1998) Crystallographic study of azurin from *Pseudomonas putida*. Acta Crystollogr. Sect. D **54:** 253-268

23. Brown K., Tegoni M., Prudencio M., Pereira A. S., Besson S., Moura J. J., Moura I. and Cambillau C. (2000) A novel type of copper cluster in nitrous oxide reductase. Nature Str. Biol. **7:** 191-195

24. Tsukihara T., Aoyama H., Nakashima R., Yano R. and Yoshikawa S. (1995) Structure of metal sites of oxidized bovine heart cytochrome *c* oxidase at 2.8 Å. Science **269:** 1069-1074

25. Iwata S., Ostermeier C., Ludwig B. and Michel H. (1995) Structure at 2.8 Å resolution of cytochrome *c* oxidase from *Paracoccus denitrificans*. Nature **376:** 660-669

26. Ducros V., Brzozowski A. M., Wilson K. S., Brown S. H., Ostergaard P., Schneider P., Yaver D. S., Pedersen A. H. and Davies, G. J. (1998) Crystal structure of the type-2 copper depleted laccase from *Coprinus cinereus* at 2.2 Å resolution. Nature Str. Biol. **5:** 310-316

27. Ducros V., Brzozowski A. M., Wilson K. S., Ostergaard P., Schneider P., Svendson A. and Davies G. J. (2001) Structure of the laccase from *Coprinus cinereus* at 1.68 Å resolution: evidence for different 'type 2 copper-depleted' isoforms. Acta. Crystallogr. Sect. D **57:** 333-336

28. Piontek K., Antorini M. and Choinowski, T. (2002) Crystal Structure of a laccase from the fungus *Trametes versicolor* at 1.90-Å resolution containing a full complement of coppers. J. Biol. Chem. **277:** 37663-37669

29. Bertrand T., Jolivalt C., Briozzo P., Caminade E., Joly N., Madzak, C. and Mougin C. (2002) Crystal structure of a four-copper laccase with an arylamine: insights into substrate recognition and correlation with kinetics. Biochemistry **41:** 7325-7333

30. Hakulinen N., Kruus K., Koivula A. and Rouvinen J. (2006) A crystallographic and spectroscopic study on the effect of X-ray radiation on the crystal structure of *Melanocarpus albomyces* laccase. Biochem. Biophys. Res. Commun. **350:** 929-934

31. Hakulinen N., Kiiskinen L. L., Kruus K., Saloheimo M., Paananen A., Koivula A. and Rouvinen J. (2002) Crystal structure of a laccase from *Melanocarpus albomyces* with an intact trinuclear copper site. Nature Struct. Biol. **9:** 601-605

32. Garavaglia S., Cambria M. T., Miglio M., Ragusa S., Iacobazzi V., Palmieri F., D'Ambrosio C., Scaloni A. and Rizzi M. (2004) The structure of *Rigidoporus lignosus* laccase containing a full complement of copper ions, reveals an asymmetrical arrangement for the T3 copper pair. J. Mol. Biol. **342:** 1519-1531

33. Lyashenko A. V., Bento I., Zaitsev V. N., Zhukhlistova N. E, Zhukova Y. N., Gabdoulkhakov A. G., Morgunova E. Y., Voelter W., Kachalova G. S., Stepanova E. V., Koroleva O. V., Lamzin V.

S., Tishkov V. I., Betzel C., Lindley P. F. and Mikhailov A. M. (2006) X-ray structural studies of the fungal laccase from *Cerrena maxima*. J. Biol. Inorg. Chem. **11:** 963-973

34. Enguita F. J., Martins L. O., Henriques A. O. and Carrondo M. A. (2003) Crystal structure of a bacterial endospore coat component: a laccase with enhanced thermostability properties. J. Biol. Chem. **278:** 19416-19425

35. Enguita F. J., Marcal D., Martins L. O., Grenha R., Henriques A. O., Lindley P. F. and Carrondo M. A. (2004) Substrate and dioxygen binding to the endospore coat laccase from *Bacillus subtilis*. J. Biol. Chem. **279:** 23472-23476

36. Bento I., Martins L. O., Lopes G. G., Carrondo M. A. and Lindley P. F. (2005) Dioxygen reduction by multi-copper oxidases; a structural perspective. Dalton Trans. 3507-3513

37. Roberts S. A., Weichsel A., Grass G., Thakali K., Hazzard J. T., Tollin G., Rensing C. and Montfort W. R. (2002) Crystal structure and electron transfer kinetics of CueO, a multicopper oxidase required for copper homeostasis in *Escherichia coli*. Proc. Natl. Acad. Sci. USA **99:** 2766-2771

38. Roberts S. A., Wildner G. F., Grass G., Weichsel A., Ambrus A., Rensing C. and Montfort W. R. (2003) A labile regulatory copper ion lies near the T1 copper site in the multicopper oxidase CueO. J. Biol. Chem. **278:** 31958-31963

39. Li X., Wei Z., Zhang M., Peng X., Yu G., Teng M. and Gong, W. (2007) Crystal structures of *E. coli* laccase CueO at different copper concentrations. Biochem. Biophys. Res. Commun. **354:** 21-26

40. Taylor A. B., Stoj C. S., Ziegler L., Kosman D. J. and Hart P. J. (2005) The copper-iron connection in biology: structure of the metallo-oxidase Fet3p. Proc. Natl. Acad. Sci. USA **102:** 15459-15464

41. Smith A. W., Camara-Artigas A., Wang M., Allen J. P. and Francisco W. A. (2006) Structure of phenoxazinone synthase from *Streptomyces antibioticus* reveals a new type 2 copper center. Biochemistry **45:** 4378 – 4387

42. Messerschmidt A., Ladenstein R., Huber R., Bolognesi M., Avigliano L., Petruzzelli R., Rossi A. and Finazzi-Agro A. (1992) Refined crystal structure of ascorbate oxidase at 1.9 Å resolution. J.

Mol. Biol. **224:** 179-205

43. Messerschmidt A., Luecke H. and Huber R. (1993) X-ray structures and mechanistic implications of three functional derivatives of ascorbate oxidase from zucchini. Reduced, peroxide and azide forms. J. Mol. Biol. **230:** 997-1014
44. Zaitseva I., Zaitsev V., Card G., Moshkov K., Bax B., Ralph A. and Lindley P. (1996) The X-ray structure of human serum ceruloplasmin at 3.1 Å: nature of the copper centres. J. Biol. Inorg. Chem. **1:** 15-23
45. Bento I., Peixoto C., Zaitsev V. N. and Lindley P. F. (2007) Ceruloplasmin revisited: structural and functional roles of various metal cation-binding sites. Acta Crystallogr. Sect. D **63:** 240-248
46. Takahashi N., Ortel T. L. and Putnum F. W. (1984) Single chain structure of ceruloplamsin: the complete amino acid sequence of the whole molecule. Proc. Natl. Acad. Sci. USA **81:** 390-394
47. Machczynski M. C., Vijgenboom E., Samyn B. and Canters G. W. (2004) Characterization of SLAC: a small laccase from *Streptomyces coelicolor* with unprecedented activity. Prot. Sci. **13:** 2388-2397
48. Adman E. T., Godden J. W. and Turley S. (1995) The structure of copper-nitrite reductase from *Achromobacter cycloclastes* at five pH values with NO_2^- bound and with type II copper depleted. J. Biol. Chem. **270:** 27458-27474
49. Inoue T., Gotowda M., Deligeer, Kataoka K., Yamaguchi K., Suzuki S., Watanabe H., Gohow M. and Kai Y. (1998) Type I copper structure of blue nitrite reductase from *Alcaligenes xylosoxidans* GIFU 1051 at 2.05 Å: resolution comparison of blue and green nitrite reductases. J. Biochem. **124:** 876-879
50. Xie Y., Inoue T., Miyamoto, Y., Matsuura H., Kataoka K., Yamaguchi K., Suzuki S. and Kai Y. (2005) Structural reorganization of copper binding site involving Thr^{15} of mavicyanin from *Cucurbita pepo medullosa* (Zucchini) upon reduction. J. Biochem. **137:** 455-461
51. Suzuki S., Kataoka K., Yamaguchi K., Inoue T. and Kai Y. (1999) Structure-function relationship of copper-containing nitrite reductase. Coord. Chem. Rev. **190-192:** 245-265
52. Suzuki S., Kataoka K. and Yamaguchi K. (2000) Metal coordination and mechanism of multicopper nitrite reductase. Acc. Chem. Res. **33:** 728-735

53. Palmer A. E., Szilagyi R. K., Cherry J. R., Jones A., Xu F. and Solomon E. I. (2003) Spectroscopic characterization of the Leu513His variant of fungal laccase: effect of increased axial ligand interaction on the geometric and electronic structure of the type I copper site. Inorg. Chem. **42:** 4006-4017

54. Xu F., Berka R. M., Wahleithner J. A., Nelson B. A., Shuster J. R., Brown S. H., Palmer A. E. and Solomon E. I. (1998) Site-directed mutations in fungal laccase: effect on redox potential, activity and pH profile. Biochem. J. **334:** 63-70

55. Sakurai T. and Suzuki S. (1997) Spectroscopy of cucumber ascorbate oxidase and fungal laccase in lit. 5 chap. 5, pp. 225-250

56. Kataoka K., Kitagawa R., Inoue M., Naruse D., Sakurai T. and Huang H. (2005) Point mutations at the type I copper ligands, Cys457 and Met467, and the putative proton donor, Asp105, in *Myrothecium verrucaria* bilirubin oxidase and reactions with dioxygen. Biochemistry **44:** 7004-7012

57. Palmer A. E., Quintanar L., Severance S., Wang T.-P., Kosman D. J. and Solomon E. I. (2002) Spectroscopic characterization and O_2 reactivity of the trinuclear copper cluster of mutants of the multicopper oxidase Fet3p. Biochemistry **41:** 6438-6448

58. Ueki Y., Inoue M., Kurose S., Kataoka K. and Sakurai T. (2006) Mutations at Asp112 adjacent to the trinuclear copper center in CueO as the proton donor in the four-electron reduction of dioxygen. FEBS Lett. **580:** 4069-4072

59. Farrar J. A., Neese F., Lappalainen P., Kroneck P. M. H., Saraste M., Zumft W. G. and Thomson J. A. (1996) The electronic structure of copper A: a novel mixed-valence dinuclear copper electron-transfer center. J. Am. Chem. Soc. **118:** 11501-11514

60. Farrar J. A., Zumft W. G. and Thomson A. J. (1998) Cu_A and Cu_Z are variants of the electron transfer center in nitrous oxide reductase. Proc. Natl. Acad. Sci. USA **95:** 9891-9896

61. Shimizu A., Sasaki T., Kwon J. H., Odaka A., Satoh T., Sakurai N., Sakurai T., Yamaguchi S. and Samejima T. (1999) Site-directed mutagenesis of a possible type I copper ligand of bilirubin oxidase; a Met467Gln mutant show stellacyanin-like properties. J. Biochem. **125:** 662-668

62. Kataoka K., Yamaguchi K., Sakai S., Takagi K. and Suzuki S. (2003) Characterization and

function of Met150Gln mutant of copper-containing nitrite reductase from *Achromobacter cycloclastes* IAM1013. Biochem. Biophys. Res. Commun. **303:** 519-524

63. Durao P., Bento I., Fernandes A. T., Melo E. P., Lindley P. F. and Martins L. O. (2006) Perturbations of the T1 copper site in the CotA laccase from *Bacillus subtilis*: structural, biochemical, enzymatic and stability studies. J. Biol. Inorg. Chem. **11:** 514-527
64. Shimizu A., Kwon J.-H., Sasaki, T., Satoh T., Sakurai N., Sakurai T., Yamaguchi S. and Samejima T. (1999) *Myrothecium verrucaria* bilirubin oxidase and its mutants for potential copper ligands. Biochemistry **38:** 3034-3042
65. Xu F., Palmer A. E., Yaver D. S., Berka R. M., Gambetta G. A., Brown S. H. and Solomon E. I. (1999) Targeted mutations in a *Trametes villosa* laccase. J. Biol. Chem. **274:** 12372-12375
66. Sakurai T., Zhang L., Fujita T., Kataoka K., Shimizu A., Samejima T. and Yamaguchi S. (2003) Authentic and recombinant bilirubin oxidase are in different resting forms. Biosci. Biotechnol. Biochem. **67:** 1157-1159
67. Arciero D. M., Pierce B. S., Hendrich M. P. and Hooper A. B. (2002) Nitrosocyanin, a red cupredoxin-like protein from *Nitrosomonas europaea*. Biochemistry **41:** 1703-1709
68. Neese F., Zumft W. G., Antholine W. E. and Kroneck P. M. H. (1996) The purple mixed-valence Cu_A center in nitrous-oxide reductase: EPR of the copper-63-, copper-65-, and both copper-65- and [^{15}N]histidine-enriched enzyme and a molecular orbital interpretation. J. Am. Chem. Soc. **118:** 8692-8699
69. Woodruff W. H., Dyner R. B. and Schoonover J. R. (1988) Resonance Raman spectroscopy of blue copper proteins. In: Biological applications of Raman spectroscopy. Chap. 9. Spiro T. G. (ed.) John Wiley & Sons, New York
70. Shimizu A., Samejima T., Hirota S., Yamguchi S., Sakurai N. and Sakurai T. (2003) Type III copper mutants of *Myrothecium verrucaria* bilirubin oxidase. J. Biochem. **133:** 767-772
71. Palmer A. E., Randall D. W., Xu F. and Solomon E. I. (1999) Spectroscopic studies and electronic structure description of the high potential type I copper site in fungal laccase: insight into the effect of the axial ligand. J. Am. Chem. Soc. **121:** 7138-7149
72. Alvarez M. L., Ai J., Zumft W. G., Sanders-Loehr J. and Dooley D. M. (2001) Characterization

of the copper-sulfur chromophores in nitrous oxide reductase by resonance Raman spectroscopy: evidence for sulfur coordination in the catalytic cluster. J. Am. Chem. Soc. **123:** 576-587

73. Cole J. L., Tan G. O., Yang E. K., Hodgson K. O. and Solomon E. I. (1990) Reactivity of the trinuclear copper active site with dioxygen: an X-ray absorption edge study. J. Am. Chem. Soc. **112:** 2243-2249

74. Sakurai T., Suzuki A. and Sano M. (1988) X-ray absorption study on the type II copper depleted cucumber ascorbate oxidase. Inorg. Chim. Acta **152:** 3-4

75. Charnock J. M., Dreusch A., Korner H., Neese F., Nelson J., Kannt A., Michel H., Garner C. D., Kroneck P. H. M. and Zumft W. G. (2000) Structural investigations of the copper A centre of nitrous oxide reductase from *Pseudomonas stutzeri* by sit-directed mutagenesis and X-ray absorption spectroscopy. Eur. J. Biochem. **267:** 1368-1381

76. Nakamura T. (1958) Purification and physico-chemical properties of laccase. Biochim. Biophys. Acta **30:** 44-52

77. Deinum J. and Vanngard T. (1973) The stoichiometry of the paramagnetic copper and the oxidation-reduction potentials of type I copper in human ceruloplasmin. Biochim. Biophys. Acta **310:** 321-330

78. Kawahara K., Suzuki S., Sakurai T. and Nakahara A. (1984) Characterization of cucumber ascorbate oxidase and its reaction with hexacyanferrate(II). Arch. Biochem. Biophys. **241:** 179-186

79. Sakurai T. (1996) Cyclic voltammetry of cucumber ascorbate oxidase. Chem. Lett. 481-482

80. Yaropolov A. I., Kharybin A. N., Emneus J., Marko-Varga G. and Gorton L. (1996) Electrochemical properties of some copper-containing oxidases. Bioelectrochem. Bioener. **40:** 49-57

81. Tsujimura S., Kano K. and Ikeda T. (2005) Bilirubin oxidase in multiple layers catalyzes four-electron reduction of dioxygen to water without redox mediators. J. Electroanal. Chem. **576:** 113-120

82. Shleev S., Tkac J., Christenson A., Ruzgas T., Yaropolov A. I., Whittaker J. W. and Gorton L.

(2005) Direct electron transfer between copper-containing proteins and electrodes. Biosens. Bioelectron. **20:** 2517-2554

83. Miura Y., Tsujimura S., Kamitaka Y., Kurose, S., Kataoka K., Sakurai T. and Kano K. (2007) Bioelectrocatalytic reduction of O_2 catalyzed by CueO from *Escherichia coli* adsorbed on a highly oriented pyrolytic graphite electrode. Chem. Lett. **36:** 132-133
84. Kamitaka Y., Tsujimura S., Kataoka K., Sakurai T., Ikeda T. and Kano K. (2007) Effects of axial ligand mutation of the type I copper site in bilirubin oxidase on direct electron transfer-type bioelectrocatalytic reduction of dioxygen. J. Electroanal. Chem. **601:** 119-124
85. Armstrong F. A. (1990) Probing metalloproteins by voltammetry. Structure and Bonding **72:** 137-221
86. Ikeda O. and Sakurai T. (1994) Electron transfer reaction of stellacyanin at a bare glassy carbon electrode. Eur. J. Biochem. **219:** 813-819
87. Sakurai T. and Nose F. (1995) Direct electrochemistry of blue copper proteins at Au electrodes modifies with promoters. Chem. Lett. 1075-1076
88. Sakurai T., Nose F., Fujiki T. and Suzuki S. (1996) Reduction and oxidation of blue copper proteins, azurin, pseudoazurin, umecyanin, stellacyanin, plantacyanin, and plastocyanin approached by cyclic and potential step voltammetries. Bull. Chem. Soc. Jpn. **69:** 2855-2862
89. Kohzuma T., Shidara S. and Suzuki S. (1994) Direct electrochemistry of nitrite reductase from *Achromobacter cycloclastes* IAM 1013. Bull. Chem. Soc. Jpn. **67:** 138-143
90. Yamaguchi K., Shuta K. and Suzuki S. (2005) Roles of Trp144 and Tyr203 in copper-containing nitrite reductase from *Achromobacter cycloclastes* IAM 1013. Biochem. Biophys. Res. Commun. **336:** 210-214
91. Fernandez C. O., Sannazzaro A. I. and Vila A. J. (1997) Alkaline transition of *Rhus vernicifera* stellacyanin, an unusual blue copper protein. Biochemistry **36:** 10566-10570
92. Nar H., Messerschmidt A., Huber R., van de Kamp M. and Canters G. W. (1991) Crystal structure analysis of oxidized *Pseudomonas aeruginosa* azurin at pH 5.5 and pH 9.0. A pH-induced conformational transition involves a peptide bond flip. J. Mol. Biol. **221:** 765-772
93. Yanagisawa S., Banfield M. J. and Dennison C. (2006) The role of hydrogen bonding at the

active site of a cupredoxin: the Phe114Pro azurin variant. Biochemistry **45:** 8812-8822

94. Sakurai T. (2006) The alkaline transition of blue copper proteins, *Cucumis sativus* plastocyanin and *Pseudomonas aeruginosa* azurin. FEBS Lett. **580:** 1729-1732

95. Battistuzzi G., Barsari M., Loschi L., Ranieri A., Sol M., Mondovi B. and Marchesini A. (2001) Redox properties and acid-base equilibria of zucchini mavicyanin. J. Inorg. Biochem. **83:** 223-227

96. Zoppellaro G., Sakurai N., Kataoka K. and Sakurai T. (2004) The reversible change in the redox state of type I copper in *Myrothecium verrucaria* bilirubin oxidase depending on pH. Biosci. Biotechnol. Biochem. **68:** 1998-2000

97. Andreasson L.-E. and Reinhammar B. (1979) The mechanism of electron transfer in laccase-catalized reactions. Biochim. Biophys. Acta **568:** 145-156

98. Hansen F. B., Noble R. W. and Ettinger M. J. (1984) Absorbance and fluorescence stopped-flow kinetics of *Rhus vernicifera* laccase and the catalytic reaction sequence. Biochemistry **23:** 2049-2056

99 O'Neill P., Filden E. M., Avigliano L., Marcozzi G., Ballini A. and Finazzi-Agro A. (1984) Pulse-radiolysis studies on the interaction of one-electron reduced species with blue oxidases. Reduction of type-2-copper depleted ascorbate oxidase. Biochem. J. **222:** 65-70

100. Kyritsis P., Messerschmidt A., Huber R., Salmon G. A. and Sykes A. G. (1993) Pulse-radiolysis studies on the oxidized form of the multicopper enzyme ascorbate oxidase: evidence for two-intramolecular electron-transfer steps. J. Chem. Soc. Dalton trans. 731-735

101. Farver O., Wherland S. and Pecht I. (1994) Intramolecular electron transfer in ascorbate oxidase in enhanced in the presence of oxygen. J. Biol. Chem. **269:** 22933-22936

102. Huang H., Zoppellaro G. and Sakurai T. (1999) Spectroscopic and kinetic studies on the oxygen-centered radical formed during four-electron reduction process of dioxygen by *Rhus vernicifera* laccase. J. Biol. Chem. **274:** 32718-32724

103. Zoppellaro G., Huang H. and Sakurai T. (2000) Kinetic studies on the reaction of the fully reduced laccase with dioxygen. Inorg. React. Mech. **2:** 79-84

104. Stoj C. S., Augustine A. J., Zeigler L., Solomon E. I. and Kosman D. J. (2006) Structural basis

of the ferrous iron specificity of the yeast ferroxidase, Fet3p. Biochemistry **45:** 12741-12749

105. Suzuki S., Furusawa H., Kataoka K., Yamaguchi K., Kobayashi K. and Tagawa S. (2000) Intramolecular electron transfer process of native and mutant forms of blue copper-containing nitrite reductase from *Alcaligenes xylosoxidans*. Inorg. React. Mech. **2:** 129-135

106. Meyer T. E., Marchesini A., Cusanovich M. A. and Tollin G. (1991) Direct measurement of intermolecular electron transfer between type I and type III copper center in the multi-copper enzyme ascorbate oxidase and its type II copper-depleted and cyanide-inhibited forms. Biochemistry **30:** 4619-4623

107. Kurose S., Kataoka K., Otsuka K., Tsujino Y. and Sakurai T. (2007) Promotion of laccase activities of *Escherichia coli* cuprous oxidase CueO by deleting the segment covering the substrate binding site. Chem. Lett. **36:** 232-233

108. Takeda T., Itoh H., Yoshioka I., Yamamoto, M., Misaki H., Kajita S., Shirai K., Kata M., Shin T., Murao S. and Tsukagoshi N. (1998) Cloning of a thermostable ascorbate oxidase from *Acremonium* sp. HI-25 and modification of the azide sensitivity of the enzyme by site-directed mutagenesis. Biochim. Biophys. Acta **1388:** 444-456

109 Bielli P., Bellench G. C. and Calabrese L. (2001) Site-directed mutagenesis of human ceruloplasmin. Production of a proteolytically stable protein and structure-activity relationships of type 1 sites. J. Biol. Chem. **276:** 2678-2685

110. Li X., Wei Z., Zhang M., Peng X., Yu G., Teng M. and Gong W. (2007) Crystal structures of *E. coli* laccase CueO at different copper concentrations. Biochem. Biophys. Res. Commun. **354:** 21-24

111. Askwith C. C. and Kaplan J. (1998) Site-directed mutagenesis of the yeast multicopper oxidase Fet3p. J. Biol. Chem. **273:** 22415-22419

112. Stoj C., Augustine A. J., Solomon E. I. and Kosman, D. J. (2007) Structure-function analysis of the cuprous oxidase activity in Fet3p from *Saccharomyces cerevisiae*. J. Biol. Chem. **282:** 7861-7868

113. Kwok E. Y., Severance S. and Kosman D. J. (2006) Evidence for iron channeling in the Fet3p-Ftr1p high-affinity iron uptake complex in the yeast plasma membrane. Biochemistry **45:**

6317-6327

114. di Patti M. C. B., Felice M. R., De Domenico I., Lania A., Alaleona F. and Musci G. (2005) Specific aspartate residues in FET3 control high-affinity iron transport in *Saccharomyces cerevisiae*. Yeast **22:** 677-687

115. Quintanar L., Stoj C., Wang T.-P., Kosman D. J. and Solomon E. I. (2005) Role of aspartate in the decay of the peroxide intermediate in the multicopper oxidase Fet3p. Biochemistry **44:** 6081-6091

116. Blackburn N. J., Ralle, M., Hassett, R. and Kosman D. J. (2000) Spectroscopic analysis of the trinuclear cluster in the Fet3 protein from yeast, a multicopper oxidase. Biochemistry **39:** 2316-2324

117. Yamaguchi K., Tsuda A., Nojiri M. and Suzuki S. (2006) Effect of arginine at type 2 copper site on spectroscopic features and enzymatic activity of copper-containing nitrite reductase. Chem, Lett. **36:** 140-141

118. Fittipaldi M., Wijma H. J., Verbeet M. P., Canters G. W., Groenen E. J. and Huber M. (2005) The substrate-bound type 2 copper site of nitrite reductase: the nitrogen hyperfine coupling of nitrite revealed by pulsed EPR. Biochemistry **44:** 15193-15202

119. Hough M. A., Ellis M. J., Antonyuk S., Strange R. W., Sawers G., Eady R. R. and Hasnain S. S. (2005) High resolution structure studies of mutants provide insights into catalysis and electron transfer processes in copper nitrite reductase. J. Mol. Biol. **350:** 300-309

120. Wijma H. J., MacPherson I., Farver, O., Tocheva E. I., Pecht I., Verbeet M. P., Murphy M. E. P. and Canters G. W. (2007) Effect of methionine ligand on the reorganization energy of the type -1 copper site of nitrite reductase. J. Am. Chem. Soc. **129:** 519-525

121. Boulanger M. J., Kukimoto M., Nishoyama M., Horinouchi S. and Murphy M. E. P. (2000) Catalytic roles for two water bridged residues (Asp-98 and His-255) in the active site of copper-containing nitrite reductase. J. Biol. Chem. **275:** 23957-23964

122. Wijma H. J., Boulanger M. J., Molon A., Fittipaldi M., Huber M., Murphy M. E. P., Verbeet M. P. and Canters, G. W. (2003) Reconstitution of the type-1 active site of the H145G/A variants of nitrite reductase by ligand insertion. Biochemistry **42:** 4075-4983

123. Zhao Y., Lukoyanov D. A., Toropov Y. V., Wu K., Shapleigh J. P. and Scholes C. P. (2002) Catalytic function and local proton structure at the type 2 copper of nitrite reductase: the correlation of enzymatic pH dependence, conserved residues, and proton hyperfine structure. Biochemistry **41:** 7464-7474

124. Kataoka K., Furusawa H., Takagi K., Yamaguchi K. and Suzuki S. (2000) Functional analysis of conserved aspartate and histidine residues located around type 2 copper site of copper-containing nitrite reductase. J. Biochem. **127:** 345-350

125. Kukimoto M., Nishiyama M., Tanokura M., Adman E. T. and Horinouchi S. (1996) Studies on protein-protein interaction between copper-containing nitrite reductase and pseudoazurin from *Alcaligenes faecalis* S-6. J. Biol. Chem. **271:** 13680-13683

126. Prudencio M., Eady R. R. and Sawers G. (2001) Catalytic and spectroscopic analysis of blue copper-containing nitrite reductase mutants altered in the environment of the type 2 copper centre: implications for substrate interaction. Biochem. J. **353:** 259-266

127. Boulanger M. J. and Murphy M. E. P. (2001) Alternate substrate binding models to two mutant (D98N and H255N) forms of nitrite reductase from *Alcaligenes faecalis* S-6: structure model of a transient catalytic intermediate. Biochemistry **40:** 9132-9241

128. Prudencio M., Sawers G., Fairhurst S. A., Yousafzai F. K. and Eady R. R. (2002) *Alcaligenes xylosoxidans* dissimilatory nitrite reductase: alanine substitution of the surface-exposed histidine 139 ligand on the type I copper center prevents electron transfer to the catalytic center. Biochemistry **41:** 3430-3438

129. Olesen K., Veselov A., ZhaoY., Wang Y., Danner B., Scholes C. P. and Shapleigh J. P. (1998) Spectroscopic, kinetic, and electrochemical characterization of heterologously expressed wild-type and mutant forms of copper-containing nitrite reductase from *Rhodobacter sphaeroides* 2.4.3. (1998) Biochemistry **37:** 6086-6094

130. Veselov A., Olesen K., Sienkiewicz, A., Shapleigh J. P. and Scholes C. P. (1998) Electronic structural information from Q-band ENDOR on the type 1 and type 2 copper liganding environment in wild-type and mutant forms of copper-containing nitrite reductase. Biochemistry **37:** 6095-6105

131. Murphy M. E. P., Turley S., Kukimoto M., Nishiyama M., Hirinouchi S., Sasaki H., Tanokura M. and Adman E. T. (1995) Structure of *Alcaligenes faecalis* nitrite reductase and a copper site mutant M150E, that contains zinc. Biochemistry **34:** 12107-12117

132. Kukimoto M., Nishiyama M., Murphy M. E. P., Turley S., Adman E. T., Horinouchi S. and Beppu T. (1994) X-ray structure and site-directed mutagenesis of a nitrite reductase from *Alcaligenes faecalis* S-6: roles of two copper atoms in nitrite reduction. Biochemistry **33:** 5246-5252

133. Kataoka K., Yamaguchi K., Kobayashi M., Mori T., Bokui N. and Suzuki S. (2004) Structure-based engineering of *Alcaligenes xylosoxidans* copper-containing nitrite reductase enhances intermolecular electron transfer reaction with pseudoazurin. J. Biol. Chem. **279:** 53374-53378

134. Murphy M. E. P., Turley S. and Adman E. T. (1998). On the mechanism of nitrite reductase: complex between pseudoazurin and nitrite reductase from *A. cycloclastes*. In: Biological electron transfer chains: genetics, composition, and mode of operation. pp. 115-128, Canters G. W. and Vijgenboom E. (eds.). NATO Science Series, Kluwer Academic Publishers, Dordrecht

135. Murphy L. M., Dodd F. E., Yousafzai F. K., Eady R. R. and Hasnain S. S. (2002) Electron donation between copper containing nitrite reductases and cupredoxins: the nature of protein-protein interaction in complex formation. J. Mol. Biol. **315:** 859-871

Figure Legends

Figure 1. Homology of amino acid sequences around the copper binding sites of multicopper oxidase, nitrite reductase, blue copper protein, nitrous oxide reductase and cytochrome *c* oxidase. 1, 2, 3, and asterisk represent type I copper ligand, type II copper ligand, type III copper ligand and proton donor, respectively. Plus represents the five amino acids shown in parenthesis. BO, bililubin oxidase; RvLc, *Rhus vernicifera* laccase; CpAO, *Cucurbita pepo* ascorbate oxidase; TvLc, *Trametes versicolor* laccase; CcLc, *Coprinus cinerius* laccase; SLAC, small laccase from *Streptomyces coelicolor*; hCp, human ceruloplasmin; AxNIR, *Alcaligenes xylosoxidans* nitrite reductase; AcNIR, *Achromobacter cycloclastes* nitrite reductase; AfNIR, *Alcaligenes faecalis* nitrite reductase; CrPC, *Chlamydomonas reinhardtii* plastocyanin; PnPc, *Populus nigra* plastocyanin, AcPAz, *Achromobacte*r *cycloclastes* pseudoazurin; PdAm, *Paracoccus denitrificans* amicyanin; TfRc, *Thiobacillus ferroxidans* rusticyanin; CsStc, *Cucumis sativus* stellacyanin; CpMv; *Cucurbita pepo* mavicyanin; PdN_2OR, *Paracoccus denitrificans* nitrous oxide reductase; AcN_2OR, *Achromobacter cycloclastes* nitrous oxide reductase; PdCOX, *Paracoccus denitrificans* cytochrome *c* oxidase; bCOX, bovine hart cytochrome *c* oxidase.

Figure 2. Structure and properties of the type I copper center and related copper centers: blue copper center, red copper center and Cu_A center.

Figure 3. X-ray crystal structure of *Trametes versicolor* laccase whose three domains are colored light pink, light green, and light blue. Figure was constructed with PyMol for Protein Data Bank (PDB) data, 1GYC.

Figure 4. Structures of the active site of CeuO (A, PDB code, 1N68), mavicyanin (B, 1WS7), and AxNIR (C, 1BQ5) showing how ligand groups are correlated with each other.

Figure 5. Absorption, CD, and EPR spectra of a multicopper oxidase, CueO (solid line) and a blue copper protein, azurin 1 from *Alcaligenes xylosoxidans* (dotted line).

Figure 6. Direct electrochemical process of multicopper oxidase, which involves an oriented association of the MCO molecule on the electrode surface, the electron transfer from electrode to type I copper center, the succeeding electron transfer to the trinuclear copper center, and the four-electron reduction of dioxygen with the concomitant supply of four protons.

Figure 7. Redox potential diagram of multicopper oxidase representing electron transfer from substrate to dioxygen and modification of the redox potential of the type I copper center by mutation.

Table 1. Blue copper center, type I copper center and variant with their donor set and redox potential

Type of Cu	Protein	Donor for Cu	Redox potential (mV vs. normal hydrogen electrode)
blue Cu center	plastocyanin	1Cys2His1Met	350-370
	azurin	1Cys2His1Met	266-305
	pseudoazurin	1Cys2His1Met	260-269
	amicyanin	1Cys2His1Met	294
	rusticyanin	1Cys2His2Met	680
	auracyanin	1Cys2His2Met	
	halocyanin	1Cys2His1Met	183 (highly pH dependent)
	plantacyanin(CBP)	1Cys2His1Met	317
	umecyanin	1Cys2His1Gln	283
	mavicyanin	1Cys2His1Gln	285
	stellacyanin	1Cys2His1Gln	180-260
red Cu center	nitrosocyanin	1Cys2His1Glu1H_2O	85
Cu_A	cytochrome *c* oxidase	2Cys2His1Met1Glu	260
	nitrous oxide reductase	2Cys2His1Met1Glu	260
type I Cu center	plant laccase	1Cys2His1Met	394
	ascorbate oxidase	1Cys2His1Met	344-370
	CueO	1Cys2His1Met	364
	PcoA	1Cys2His1Met	
	CumA, MofA, MnxG	1Cys2His1Met	
	EpoA	1Cys2His1Met	
	CotA	1Cys2His1Met	455
	dihydrogeodin oxidase (sulochrin oxidase)	1Cys2His1Met	
	nitrite reductase	1Cys2His1Met	240-260
	hephaestin	1Cys2His1Met	
	ceruloplasmin	1Cys2His1Met/1Leu	490, 580, >1000
	phenoxazinone synthase	1Cys2His1Met	
	bilirubin oxidase	1Cys2His1Met	680
	Fet3p	1Cys2His1Leu	433
	fungal laccase	1Cys2His1Phe/Leu	550-785

Table 2. X-ray crystallographic data of multicopper proteins

Multicopper protein	X-ray crystallographic characterization with Protein Data Bank (PDB) code or lit.
ascorbate oxidase	ox. form (1AOZ), red. form (1ASO), peroxide-incubated (1ASP), azide-incubated (1ASQ), ascorbate-incubated [42]
CueO	ox. form (1KV7), Cu-soaked (1N68), M441L (1PF3), Δα5–7 (2YXV), Δα5–7 Cu-incubated (2YXW), low Cu amount form (2FQD, 2FQE, 2FQF, 2FQG)
CotA	ox. form (1GSK), red. form (2BHF), SGZ-incubated (1HKP, 1HL0), ABTS-incubated (1HKZ, 1HL1, 1OGR), EBS-soaked (1OF0), ABTS-adduct (1UVW), $CuCl_2$-incubated (1W6L), azide-incubated (1W6W), peroxide-incubated (1W8E), M502L/F [63]
phenoxazinone synthase	ox. form (2G23)
Fet3p	ox. form (1ZPU)
fungal laccase	*Coprinus cinereus*: T2D (1A65, 1HFU) *Melanocarpus almomyces*: ox. form (1GW0, 2IH8, 2IH9) *Trametes versicolor*: ox. form (1GYC), 2,5-xylidine-complexed (1KYA) *Rigidoporus lignosus*: ox. form (1V10) *Cerrena maxima*: ox. form (2H5U)
ceruloplasmin	ox. form (1KCW, 2J5W)
nitrite reductase	*Alcaligenes faecalis*: ox. form (1AS6, 1AS7, 1QEO1, 2AVF), half-apo (1QE3), red. form (1AO8, 2FJS), nitrite-bound, (1AS8, 1SJM), NO-bound (1SNR), A98N (1ET5),H255D (1ET7, 1ET8), H255N (1J9S, 1JQT), D98N (1J9O, 1JQR), I257A (1L9O), I257G (1L9P), I257L (1L9O), I257M (1L9R), I257T (1L9S), I257V (1L9T), H145A (1NPJ, 1NPN), M150E (1NTD, 2AFN), D92E (1QE2), M150G (1ZDO, 1ZDS, 2B08) , M168L (2BP0), M168Q (2BP8) *Alcaligenes xylosoxidans*: ox. form (1BO5, 1NDR, 1NDT), apo, high pH (1HAU, 1HAW), M144A (1GS6), H254F (1GS7), D92N (1GS8), W138H (1WA0), H313Q (1WA1, 1WA2), H129V (1WAE), nitrite-bound (1NDS) *Rhotobacter sphaeroides*: ox. form (1ZV2, 2A3T, 2DY2), M182T (1MZY, 1MZZ), H287A (1N70), nitrite-bound (2DWS, 2DWT) *Achromobacter cycloclastes*: ox. form (1RZP, 1RZP, 2BW4), nitrite-bound T2D (1NIA~1NIE, 2BWI, 2NRD), NO-bound (2BW5, 2BWD), I257E (1KCB) *Hyphomicrobium denitrificans*: ox. from (2DV6)

Δα5–7, helices 5-7 were deleted; SGX, syrinagaldazine; EBS, 3-ethyl-2-[(2Z)-2-(3-ethyl-6-sulfo-1,3-benzothiazole-2(3H)-ylidene)hydrazino]-6-sulfo-3H-1,3-benzothiazole-1-ium; T2D, type 2 Cu depleted.

Table 3. Mutants of multicopper proteins

Multicopper protein	Mutant	Reference
ascorbate oxidase	T1: M544I, other site: A565I/S/V/L/G/T/M/N/D/E, F465W, M86I, I534F, A465L/F463W, S124G/V136L, A465L/F463W/M86I, A465W/F463/I/M86/I	[108]
bilirubin oxidase	T1: M467F/L/N/G/H/R, C457A/V/S, T2: H94V/N, T3: H456,458V/K/D, H134,136V, Proton donor: D105E/N/A	[56], [61], [64], [70], [84]
ceruloplasmin	T1: C1021S, L329M	[109]
CotA	T1; M502L/F	[63]
CueO	T1: C500S, M510L/Q/A/V, proton donor: D112E/A/N, other site: E106F, deletion mutant: Δα5−7, Δα6−7, Δα5, Δα5−7+1/2α	[58], [107], [110]
Fet3p	T1: L494V/F/K/I/A/M, C484S, T1T3: C484S/H81N, T1T3: C484S/H126 N, T1T3: C484S/H128N T2: H81N, T3: H489F, proton donor: D94, Other site: E227A, D228A, E330A, M281A, M345A, M281A/M345A, E185A/D, D409A, D283A, D409A/E, E185A/D409A, D278Q, D279N, D312N, D315I, D319N, D320N	[57], [104], [111-116]
T. villosa laccase	T1: F463L/M, A461E/F463L	[65]
M. thermophila laccase	T1: L513F/H, other site: L509V/E467S/A468A	[53], [54]
R. solani laccase	T1: L470F, other site: L466V/E467S/A468G	[54]
nitrite reductase	T1: M150Q/G/T/H/E/D, M182T, M144L, H145A/G, H139A, H135K, other site: W144L, Y203L, H133R, D98A/N/E, D92E/N, H255N/D/A/K/R, D129A/N, H287A, I289A, E46S, E58A, E89S, E133A, E118A, E160A, E197A, D201A, E204A, D205A, E112A/E197A/D201A, H287E	[62], [90] [117-132]

Data on nitrous oxide reductase and cytochrome *c* oxidase were not included

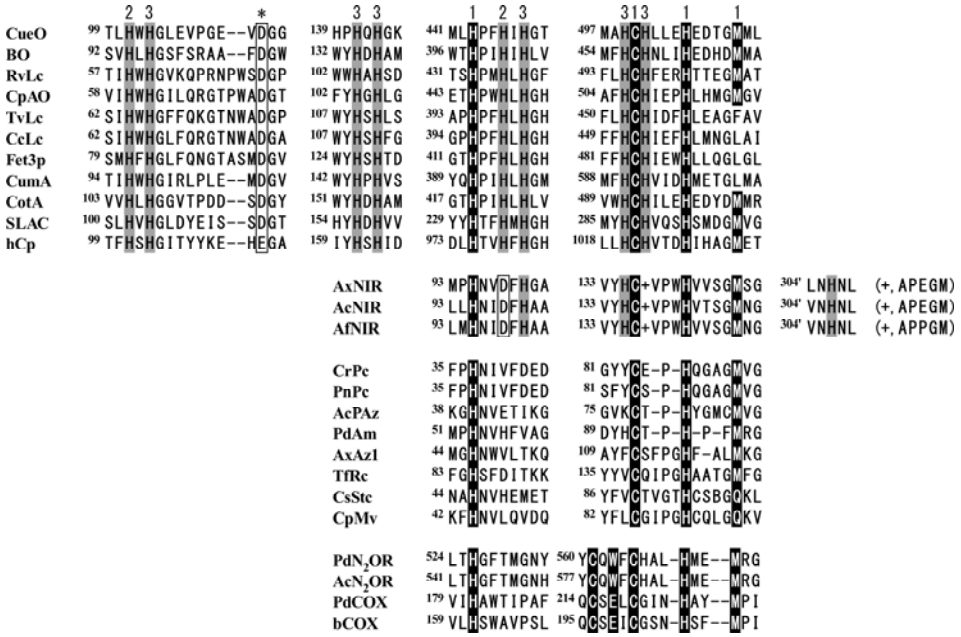
CueO
BO
RvLc
CpAO
TvLc
CcLc
Fet3p
CumA
CotA
SLAC
hCp
AxNIR
AcNIR
AfNIR
CrPc
PnPc
AcPAz
PdAm
AxAz1
TfRc
CsSte
CpMv
PdN2OR
AcN2OR
PdCOX
bCOX

Fig. 1

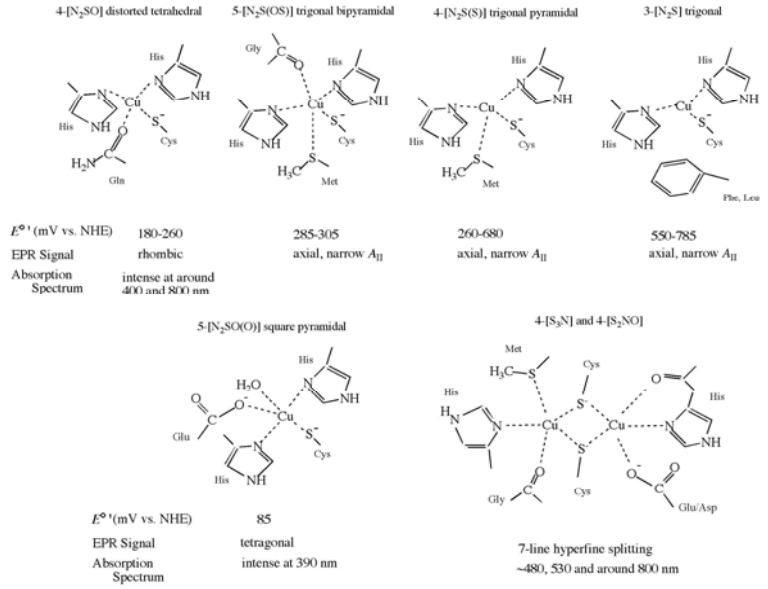
4-[N2SO] distorted tetrahedral
5-[N2S(OS)] trigonal bipyramidal
4-[N2S(S)] trigonal pyramidal
3-[N2S] trigonal
E°' (mV vs. NHE)
180-260
285-305
260-680
550-785
EPR Signal
rhombic
axial, narrow AII
axial, narrow AII
axial, narrow AII
Absorption Spectrum
intense at around 400 and 800 nm
5-[N2SO(O)] square pyramidal
4-[S2N] and 4-[S2NO]
E°' (mV vs. NHE)
85
EPR Signal
tetragonal
Absorption Spectrum
intense at 390 nm
7-line hyperfine splitting
~480, 530 and around 800 nm

Fig. 2

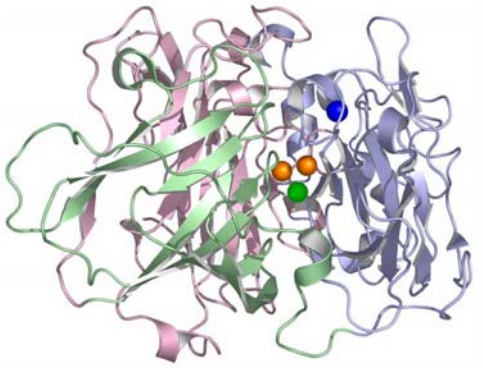

Fig. 3

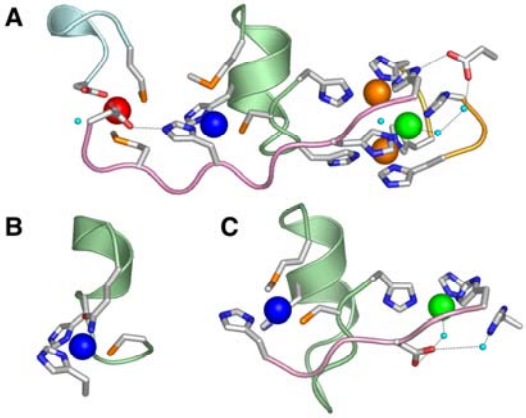

Fig. 4

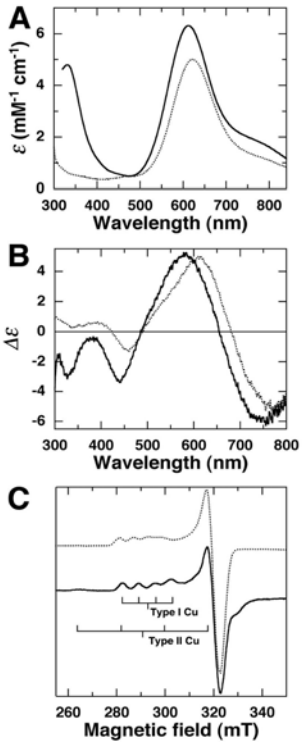

Fig. 5

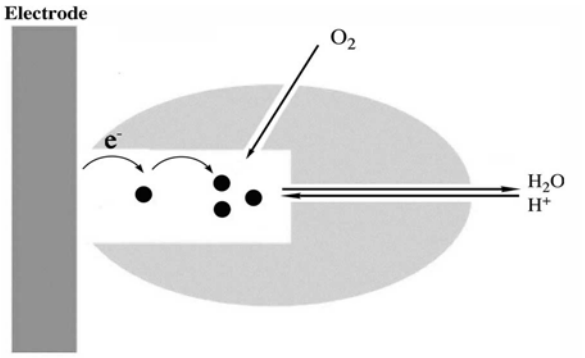
Electrode
O_2
e^-
H_2O
H^+

Fig. 6

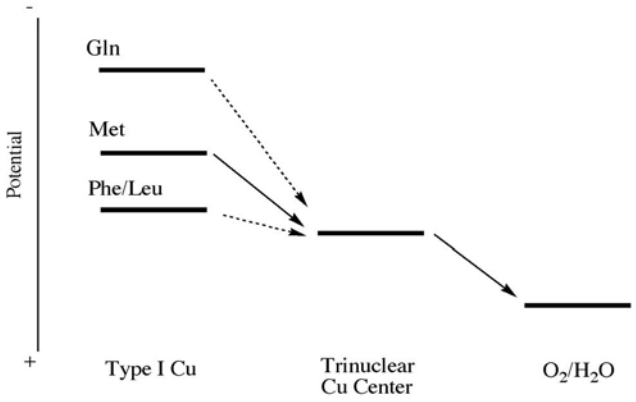
-
Gln
Met
Phe/Leu
Potential
+
Type I Cu
Trinuclear
Cu Center
O_2/H_2O

Fig. 7